Int. J. Solids Structures, 1969, Vol. 5, pp. 1221 to 1230. Pergamon Press. Printed in Great Britain

RADIAL INERTIA EFFECTS ON AN IDEALLY PLASTIC CIRCULAR PLATE UNDER IMPULSIVE AXIAL COMPRESSION

N. DAVIDS, G. PUTTAIAH and P. K. MEHTA

Department of Engineering Mechanics, The Pennsylvania State University

Abstract—An analysis is presented here of the dynamic problem of a circular rigid-perfectly-plastic plate forged between two rigid plates under a number of input conditions. It is shown that the radial inertia of the deforming plate has a significant effect, and hence the results of this dynamic solution differ for instance, for high axial strain rates from those which would have been obtained under static conditions, for which an exact mathematical solution already exists [1].

The approach used is that of finite element analysis. The analysis is applied to some cases of practical interest. Input conditions treated are (a) prescribed axial strain rate, (b) axial strain rate dependent on plate thickness and time, (c) constant forging power and (d) constant compression total force.

A previously known static solution [1] is obtained with excellent agreement, as a special case of this analysis, by taking very small axial strain rates.

NOTATION

a_r^i	acceleration of ith element
$\bar{a}_r^i$	acceleration of the c.g. of ith element
b_0	initial radius of plate
b	current radius of plate
F_i	x-component of resultant force on ith element
h_0	initial thickness of plate
h	current thickness of plate
i	cell index
m_i	mass of ith element
N	identification coefficient for dynamic and quasi-static solutions
N_1	coefficient, identifying transition from sliding to sticking at contact surface
N_2	$\left(\mu N_1 + \dfrac{1-N_1}{2}\right)(r_i - r_{i+1})$
p	axial pressure, psi
r	radial coordinate
r_i	radial coordinate of ith element
$\bar{r}_i$	radial coordinate of c.g. of ith element
r_{tr}	transition radius
t	time
v	particle velocity
v_r^i	velocity of ith element at radius r_i
$\bar{v}_r^i$	velocity of c.g. of ith element
Y	yield stress in uni-axial tension
Y_1	yield stress in shear $= Y/2$
z	axial coordinate
α	$\mu(r_i - r_{i+1})$
β	ratio of distance of mass centre to average radius of the semi ring element from centre
θ	tangential co-ordinate
ε	strain
$\dot{\varepsilon}$	strain rate

σ normal stress
τ surface shear force per unit area
λ flow parameter
μ coefficient of friction between plate and forge-head

INTRODUCTION

THE PROCESS of sudden or rapid squeezing of a plastic material between two plates has been both of basic and applied interest. If the material is in the form of a circular plate and squeezing plates are assumed rigid, we have a geometrical set-up which is simple enough to allow theoretical analysis and experimental study of the laws of plasticity involved in the lateral (i.e. radial) motion of such a material when yielded. Forging processes also are based on making optimum use of the relationships between deformation of the specimen and the form of the applied pressure.

A relation exists between this arrangement and the lateral deformation which occurs in a projectile striking a rigid target, say. This is a problem studied by Taylor [3], Lee and Tupper [4], Raftopoulos and Davids [5], and others. In the projectile problem we have one plate instead of two. However, the velocities here, which are of the order of 1000–3000 ft/sec. are high enough to bring into play lateral inertia forces in the deforming material which, as will be shown in this paper, appreciably affect the deformation.

Until now the "forging" problem has been limited to slow-deformation, i.e. static analysis. Our aim here is to show how a dynamic analysis can be made, i.e. one which includes the inertia effects, and, under high deformation rates, that the lateral inertia effects are appreciable.

1. BASIC PLASTICITY THEORY

We assume that the material is incompressible and obeys the Levy–Mises flow rule [2].

$$\dot{\varepsilon}_r/\sigma'_r = \dot{\varepsilon}_\theta/\sigma'_\theta = \dot{\varepsilon}_z/\sigma'_z \tag{1.1}$$

where $\sigma'_r, \sigma'_\theta, \sigma'_z$ are deviatoric stresses. It is further assumed that the forge heads are rigid, so that we have axial strain rates independent of r and θ, i.e.

$$\dot{\varepsilon}_z = \dot{\varepsilon}_z(t, z). \tag{1.2}$$

Then it can be shown, [1] for cylindrical symmetry, that

$$v_r = -(1/2)\dot{\varepsilon}_z r \tag{1.3}$$

and that

$$\dot{\varepsilon}_\theta = \dot{\varepsilon}_r = -(1/2)\dot{\varepsilon}_z \tag{1.4}$$

From (1.1) and (1.4)

$$\sigma_\theta = \sigma_r \tag{1.5}$$

For such a "cylindrical" stress state the yield conditions of either Tresca or Von Mises give the same relation

$$\sigma_r - \sigma_z = \sigma_\theta - \sigma_z = Y \tag{1.6}$$

and since

$$\sigma_z = -p, \tag{1.7}$$

$$\sigma_r = \sigma_\theta = Y + \sigma_z = Y - p. \tag{1.8}$$

Formulas (1.3) to (1.8) apply where $\dot{\varepsilon}_z$ is independent of r and θ.

2. FINITE ELEMENT ANALYSIS OF FORGING PROBLEM

The analysis begins by dividing up the plate into a set of semi-circular ring elements $i = 1, \dots i_m$ counted from outside inward. Figure 1 shows a sample element and the forces acting on it, shown corresponding to positive values of the stresses.

Analysis of force and stresses due to radial inertia

By Newton's law of motion, the net x-component of total force on the semi-ring is

$$F_i = m_i \bar{a}_x^i \tag{2.1}$$

where $\bar{a}_x^i$ refers to the acceleration of the c.g. of the element. This is then related geometrically to that of the element by the relation

$$\bar{a}_x^i = (\bar{R}_i/R_i)a_x^i = \beta_i a_x^i. \tag{2.2}$$

To calculate β_i we have

$$\bar{R}_i = \int (r \cos\theta)\, \mathrm{d}A/A$$

and

$$R_i = (r_{i+1} + r_i)/2$$

which, on carrying out the indicated surface integration, gives

$$\beta_i = (8/3\pi)[1 - r_i r_{i+1}/(r_{i+1} + r_i)^2]. \tag{2.3}$$

Referring to Fig. 1, we get F_i:

$$F_i = \sigma_r^i(2r_i h) - \sigma_r^{i+1}(2r_{i+1}h) - \sigma_\theta^i(2r_i - 2r_{i+1})h + F_\mu^i. \tag{a}$$

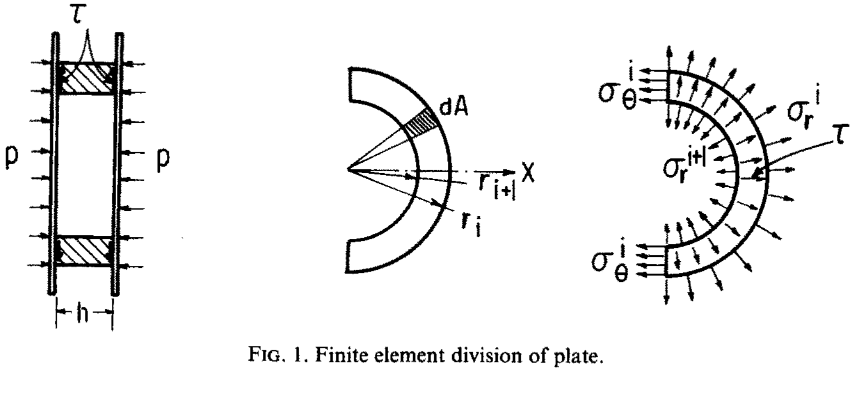

FIG. 1. Finite element division of plate.

Since σ_r is not a constant across the element, we obtain an average value for tangential stress (σ_θ) using (1.5), as follows:

$$\sigma_\theta^i = \tfrac{1}{2}(\sigma_r^{i+1} + \sigma_r^i). \tag{b}$$

Frictional contribution to x-component of force

Since the surface shearing force per unit area τ results from friction on the element, we have

$$\tau = \mu\sigma_z = -\mu p \quad \text{if } v_r \neq 0$$

$$\tau = 0 \quad \text{if } v_r = 0$$

i.e. if the element is moving outward, the friction force actually is negative. Its value is calculated as follows: Referring to Fig. 1, by integrating over the surface areas of the element normal to the axis,

$$F_\mu^i = 2\int \tau^i \cos\theta \, \mathrm{d}A = 2\mu\bar{\sigma}_z^i(r_i^2 - r_{i+1}^2) \tag{c}$$

where $\bar{\sigma}_z^i$ is the average stress on the element. From (1.6),

$$\bar{\sigma}_z^i = \tfrac{1}{2}(\sigma_r^{i+1} + \sigma_r^i) - Y$$

giving

$$F_\mu^i = \mu(\sigma_r^{i+1} + \sigma_r^i - 2Y)(r_i^2 - r_{i+1}^2). \tag{d}$$

Substituting (b) and the expression for F_μ^i (sliding only) from (d) into (a) and simplifying:

$$\sigma_r^{i+1} = [(h+\alpha_i)\sigma_r^i - 2\alpha_i Y - F_i/(r_i + r_{i+1})]/(h-\alpha_i) \tag{2.4}$$

where

$$\alpha_i = \mu(r_i - r_{i+1}). \tag{2.5}$$

In this way, an inductive relation is obtained which gives the $(i+1)$th stress from the ith value, supposedly known.

Sticking of plate. For sufficiently large normal pressure the material sticks to the forging plate and yields internally instead in shear. It can then be shown by integration, starting from the condition $Y_1 = Y/2$, that

$$F_\mu^i = -Y(r_i^2 - r_{i+1}^2). \tag{e}$$

The expression (2.4) for the radial stress, written so as to include both cases, may now be written

$$\sigma_r^{i+1} = [\sigma_r^i(h + N_1\alpha_i) - 2N_2 Y - F_i/(r_{i+1} + r_i)]/(h - N_1\alpha_i) \tag{2.6}$$

where

$$N_1 = 1 \quad \text{sliding}$$

$$N_1 = 0 \quad \text{sticking}$$

and

$$N_2 = (\mu N_1 + (1 - N_1)/2)(r_i - r_{i+1}). \tag{2.7}$$

From the yield criterion (1.8), the axial pressure is given by

$$p_i = Y - \sigma_r^i \tag{2.8}$$

New plate thickness

$$h' = h(1+\dot{\varepsilon}_z \Delta t). \tag{2.9}$$

If $\dot{\varepsilon}_z$ is prescribed as a function of time we use the average current value at t.

New radius of plate

$$r_i' = r_i + v_r^i \Delta t. \tag{2.10}$$

Thus we have shown how all the dynamical variables may be calculated at the end of the prescribed time interval Δt from their values at the beginning. In this way, after updating the time by setting

$$t' = t + \Delta t$$

we may continue this process again until any desired termination.

3. INPUT CONDITIONS

The analysis presented above was applied to a number of input conditions, as described below.

Case 1—$\dot{\varepsilon}_z$ a constant or a prescribed function of time

The steps in the procedure are as follows:

(a) from (1.3) the values of v_r^i are known at time t for all radii r_i.
(b) the accelerations of each semi-ring are calculated from (2.2).
(c) the forces F_i are then determined from (2.1).
(d) from the boundary condition $\sigma_r^i = 0$ for the outermost element, the σ_r^{i+1} are calculable from (2.6).
(e) the pressures p_i are then obtained from (2.8).
(f) the new element thickness is then obtained from (2.9).
(g) the final radius at the end of each time interval is given by (2.10).

Steps (a) to (g) are repeated for any specified number of time intervals until the forging process is terminated.

If a small value is taken for $\dot{\varepsilon}_z$, say 0·01/sec we obtain the static solution, previously known mathematically [1]. Also, if the radial inertia forces are omitted from the analysis, even though a high input rate is specified, i.e. the so-called quasi-static case, the results differ appreciably, as will be seen.

Physically, it is necessary to decrease the applied strain rate with time as the thickness of the plate becomes smaller. However, the analysis is the same as the previous one.

Case 2—$\dot{\varepsilon}_z$ a function of plate thickness

The same analysis applies for any prescribed thickness function.

Case 3—Forging power prescribed

Equating the rate of energy dissipation of a volume V of rigid-plastic material to the power supplied [2], say by the forging machine, we have

$$Fv_z = (\sigma_r' \dot{\varepsilon}_r + \sigma_\theta' \dot{\varepsilon}_\theta + \sigma_z' \dot{\varepsilon}_z)V \tag{3.1}$$

where F is the applied force and σ' the deviatoric stresses. Applying (1.5), this becomes

$$Fv_z = 2(\sigma_r - \sigma_z)\dot{\varepsilon}_r V = 2YVv_r/r$$

which gives

$$v_r = Fv_z r/2YV$$

The average velocity of the ith elementary semi-ring is

$$v_r^i = Fv_z(r_i + r_{i+1})/4YV \tag{3.2}$$

Thus, if Fv_z is given, the radial velocities of the elements can be calculated, and from this radial inertia forces obtained as previously. Since $\dot{\varepsilon}_z$ is assumed independent of radius, the remaining analysis, including determination of pressure distribution and radius of the plate is the same as in Case 1. The plate thickness is calculated from the incompressibility condition.

Case 4—Constant applied force on plate

Since the total force acting on the plate does not come into the analysis directly, an inverse iterative procedure is needed here. We start with an assumed value for $\dot{\varepsilon}_z$, then integrate the resulting pressure distribution over the plate area to obtain the total force, which is then compared with the specified value of the force. If the two differ, $\dot{\varepsilon}_z$ is altered by a suitable small increment and the process repeated until the error is less than a specified amount. The value of $\dot{\varepsilon}_z$ which gives the correct force is then used to obtain radius and thickness as in Case 1.

4. RESULTS

(a) *Numerical computation*

The analysis presented above is easily adapted for use in a computer. For the results shown here, the total number of elements i_m was 25. At first 20 elements were used, with no appreciable loss of accuracy. The time interval $\Delta t = 1\ \mu$ sec. This was found to be just as accurate as $\Delta t = 0{\cdot}5\ \mu$ sec. The total computer time averaged about 1 min on the IBM 7074 computer.

(b) *Discussion of results*

In all the results presented, quasi-static analysis (neglect of radial inertia) is compared with our dynamic analysis. They differ considerably, especially with increase of the input variable, e.g. axial strain rate or total force.

Figure 2 shows non-dimensional pressure against plate radius for very small axial strain rate. As seen, the results coincide with those obtained mathematically [1]. Figure 3 shows pressure distribution for various constant axial strain rates. The transition radius (sticking to sliding) for quasi-static differs markedly from the dynamic analysis. While the pressure is linear in the sticking zone for quasi-static case, it becomes non-linear for the dynamic case. As can be seen, pressure on the plate is strongly influenced by axial strain rate. Thus we see the importance of including the effect of radial inertia.

Figure 4 shows how axial pressure at the plate centre varies with time. Note that the pressure not only increases but accelerates with time. This is because an increasing pressure is required to maintain the constancy of the axial strain rate.

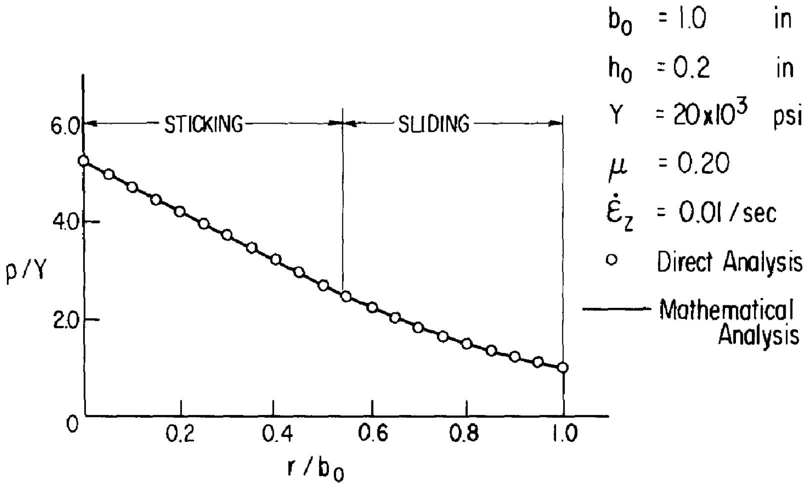

FIG. 2. Forging pressure distribution, Static case at $t = 2$ μsec.

An interesting variation of this problem is seen in Fig. 5, where we have a linearly decreasing strain rate with time. This is physically more reasonable than the constant case. For the highest rates shown ($\dot{\varepsilon}_{z0} = 25{,}000$ and $30{,}000$) the axial pressure vanishes respectively at $t = 13$ and $18{\cdot}2$ μsec and then actually goes negative, according to this analysis. This may be explained on the basis of the high radial inertia of the deforming material,

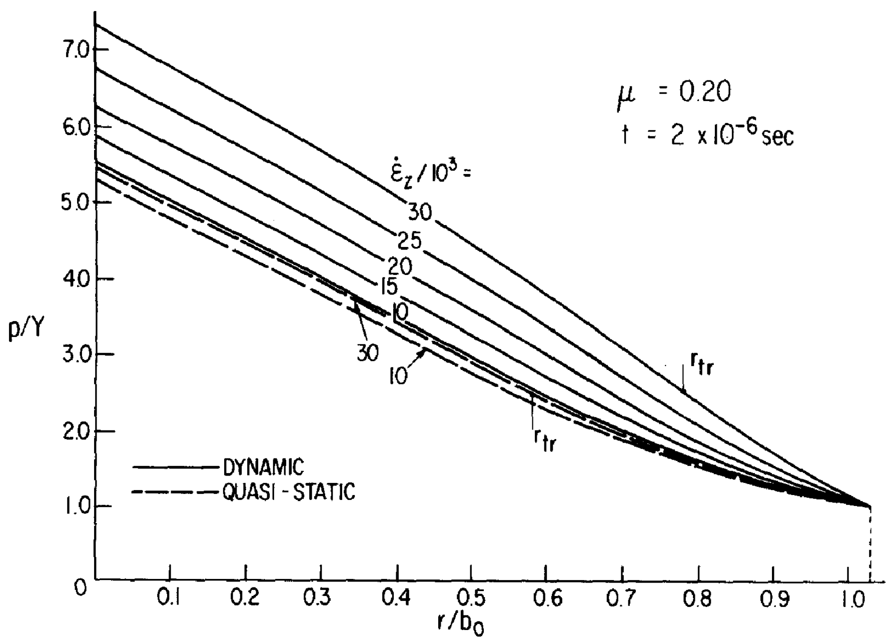

FIG. 3. Pressure profile comparison between Dynamic and Quasi-static solutions for constant Axial Strain Rate inputs at $t = 2$ μsec.

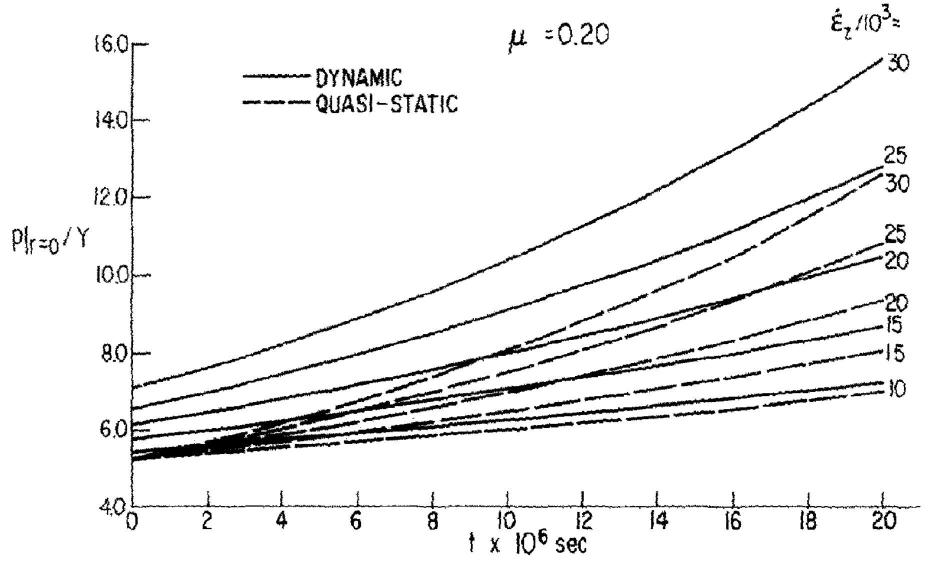

FIG. 4. Axial pressure at plate centre vs. time for Axial Strain Rates.

which tends to keep the plate thickness decreasing faster than the externally applied excitation. Of course, the actual behavior of the material under tension may be different from what we have assumed it to be.

The remaining figures (Figs. 6–8) show pressure profiles over the plate for the remaining input conditions described in this paper, e.g. where axial strain rate is a linear function of

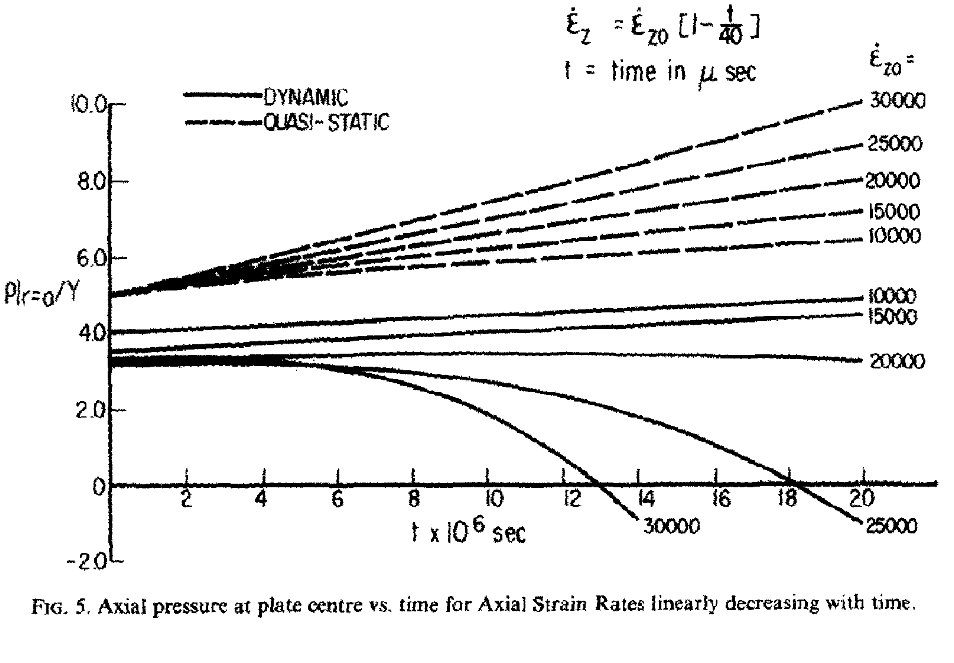

FIG. 5. Axial pressure at plate centre vs. time for Axial Strain Rates linearly decreasing with time.

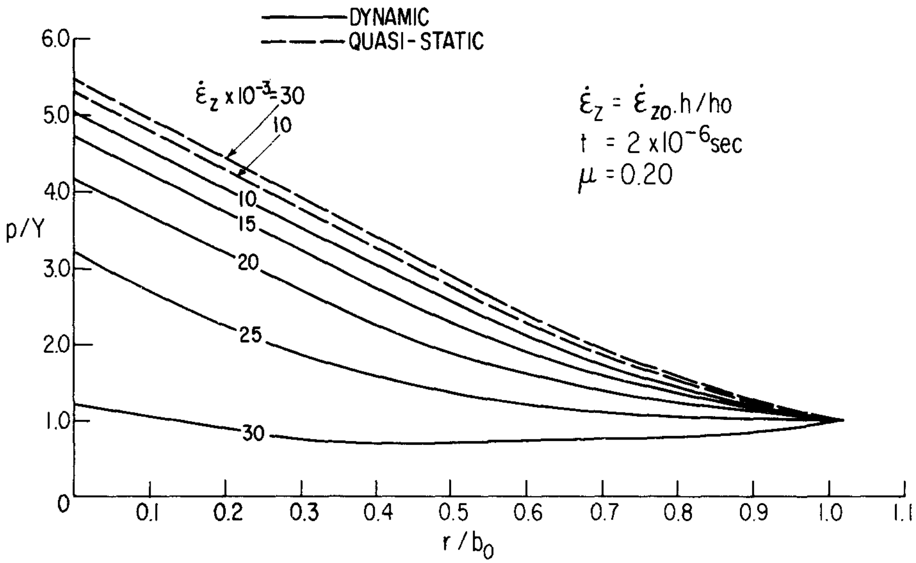

FIG. 6. Pressure profile comparison between Dynamic and Quasi-static solutions for Axial Strain Rates linearly varying with plate thickness at $t = 2$ μsec.

plate thickness, where the total axial force, and the total power are prescribed. We note that the fastest cases differ from the quasi-static result by as much as two to five times.

Further implications of the analysis become apparent if the velocities of impact are increased still further. The inertia effects analyzed here become considerably greater and may, in fact, dominate the deformation behavior of the material. Further work is being done, using this method, for free plates and for input conditions variable with radius.

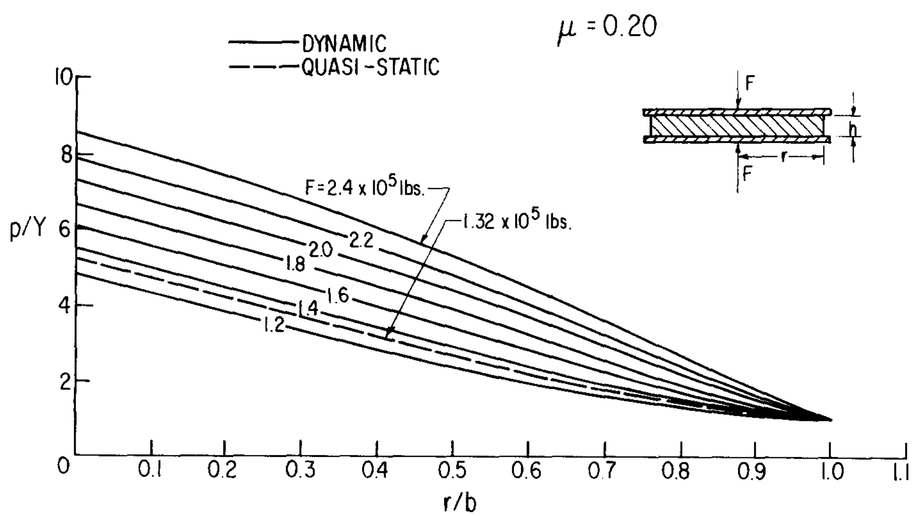

FIG. 7. Pressure profile for constant total axial force at $t = 2$ μsec.

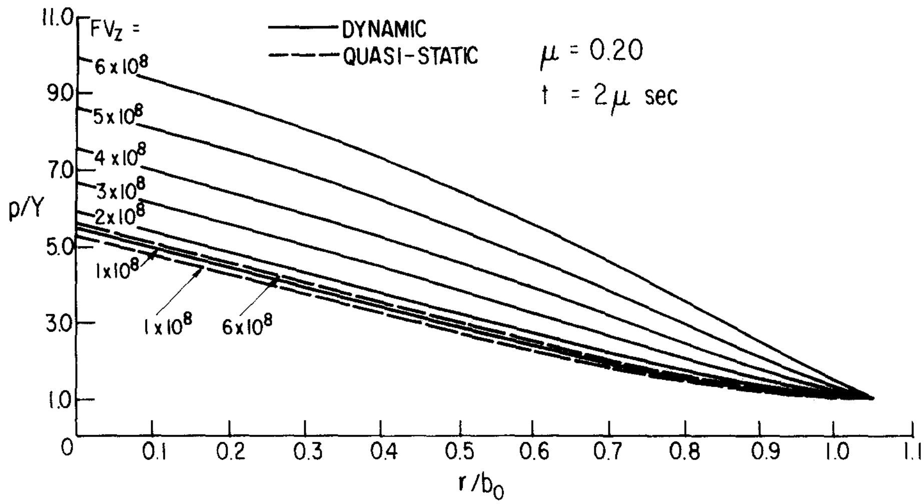

FIG. 8. Pressure profile comparison between Dynamic and Quasi-static static solutions for power inputs at $t = 2\ \mu$sec.

Acknowledgement—This work was sponsored by the Ballistic Research Laboratories, Aberdeen Proving Ground. Their support is gratefully acknowledged.

REFERENCES

[1] O. HOFFMAN and G. SACHS, *Introduction to the Theory of Plasticity*, pp. 240–248. McGraw-Hill (1953).
[2] W. JOHNSON and P. B. MELLOR, *Plasticity for Mechanical Engineers*, pp. 60, 69. Van Nostrand (1962).
[3] G. I. TAYLOR, The use of flat-ended projectiles for determining dynamic yield stress—I: Theoretical consideration. *Proc. R. Soc.* **A194**, 289 (1948).
[4] E. H. LEE and S. J. TUPPER, Analysis of plastic deformation in a steel cylinder striking a rigid target. *J. appl. Mech.* **21**, 63–70 (1954).
[5] D. RAFTOPOULOS and N. DAVIDS, Elastoplastic impact on rigid targets, *AIAA Jnl* **5**, 2254–2260 (1967).

(*Received* 28 *October* 1968; *revised* 20 *February* 1969)

Абстракт—Дается решение динамической задачи круглой, жесткоидеально-пластической пластинки, выкованной между двумя жесткими пластинами, под влиянием некоторого числа заданных условий. Показано, что радиальная инерция деформированной пластинки вызывает значительный эффект. Следовательно результаты этих динамических решений отличаются, на пример, для больших скоростей особых деформаций, от таких, которые получаются принимая во внимание статические условия, для которых уже существует точное математическое решение [I].

Используется метод расчета конечного элемента. Применяется расчет к некоторым случаям, имеющим практическое значение. Рассматриваются следующие заданные условия:

а/ заданная скорость осевой деформации,
б/ сокрость деформации зависящая от толщины пластинки и времени,
в/ постоянная сила ковки и 2/ постоянная полная сила сжатия.

Принимая очень малые скорости осевых деформаций, получается предыдущее известное статическое решение с идеальной сходимостью, рассматриваемое в качестве специального случая настоящего расчета.